Tellus (1998), 50A, 302–312
Printed in UK – all rights reserved

TELLUS
ISSN 0280–6495

The rôle of planetary waves in the formation of polar stratospheric clouds

By H. TEITELBAUM* and R. SADOURNY, *Laboratoire de Météorologie Dynamique du CNRS, École Normale Supérieure, 24, rue Lhomond, 75231 Paris Cedex 05, France*

(Manuscript received 23 June 1997; in final form 26 November 1997)

ABSTRACT

Several recent works attribute the formation of polar stratospheric clouds (PSCs) to the occurrence of localized orographic waves. Using ECMWF analyses, we investigate the large scale stratospheric flow conditions in a number of cases where PSCs have been detected, both in the Arctic and in the Antarctic. We show that PSCs appear within strong planetary scale uplifts of isentropic surfaces. The adiabatic cooling of air parcels travelling within such planetary scale uplifts while conserving their humidity and trace constituents, seems to be the main mechanism for PSC formation. The PSC distribution would then follow a planetary structure, even though local orographic waves could still play an additional role when planetary scale conditions are met.

1. Introduction

The discovery of the ozone hole over Antarctica in late winter and early spring by Farman et al. (1985) has led to considerable research on the causes responsible for this ozone deficit. The same paper (Farman et al., 1985) attributes the ozone destruction to the increase of chlorine through the increase of CFCs. Nevertheless, Rowland et al. (1986) have shown that direct homogeneous reactions involving these compounds play a negligible part in the process. On the other hand, Molina et al. (1987), Tolbert et al. (1987) and other authors have shown that the reactions leading to active chlorine are most rapid and efficient when they take place on ice surfaces. This is precisely the case in the atmosphere when polar stratospheric clouds (PSCs) are present, and currently the Antarctic ozone destruction is well explained by heteregeneous reactions of chlorine compounds occurring on PSCs (Solomon et al., 1986; Crutzen and Arnold, 1986; Molina and Molina, 1987).

* Corresponding author.

PSCs have indeed been observed for more than a century. More recent observations by the SAM-II satellite system show some details of their temporal and spatial distribution (McCormick et al., 1981). For example, at all altitudes and for all years, many more PSCs are observed in the Antarctic than in the Arctic, a consequence of the colder temperature of the Antarctic stratospheric air.

In general the formation of PSCs needs air temperatures of about 190 K. Toon et al. (1986) and Crutzen and Arnold (1986) suggested that PSCs might begin to form at temperatures above the frost point as mixtures of nitric acid and water, namely nitric acid trihydrate (NAT) formed by three water molecules associated with one molecule of nitric acid. PSCs are classified in two broad categories: Type I PSCs which are formed of NAT and begin to appear at 195 K, and Type II PSCs which are composed of water and are less frequently found because they cannot form above 188 K. The formation time scale also depends on the PSC type (Turco et al., 1989). Type I PSCs form in approximately 10^5 s, whereas Type II formation only needs 10^3 to 10^4 s.

Even in the Antarctic where the temperature is approximatively 5 K lower than in the Arctic, PSCs are not a permanent feature of the stratosphere. Their generation needs a mechanism able to bring air temperature down to the above threshold values. According to Cariolle et al. (1989), one possible mechanism is the adiabatic cooling due to vertical motion induced by mountain waves. This proposal was based on observations obtained during the airborne Antarctic ozone experiment (AAOE), showing that clouds are preferentially located above the Palmer peninsula. Nevertheless, even though mountain waves can be involved, it is not obvious that they are the dominant process. In a stationary mountain wave structure, air masses will go up and down with a period of less than an hour, too short to allow formation of most PSCs unless some hysteresis process is also involved, which has yet to be demonstrated.

In this paper, we shall show a number of cases where the primary mechanism producing the adiabatic cooling needed for PSC formation is upward motion induced by planetary waves. Our work is based on PSC measurements reported in the existing literature, and on analyses ot the European Center of Medium Weather Forecast (ECMWF). Some of the measurements have been performed by ground-based or aircraft-borne lidars, some are obtained in situ by balloon borne instruments. The various techniques involved can be found from the referenced papers.

In section 2 we explain the invoked mechanism, which we extensively illustrate by an example from the Arctic winter. Section 3 reviews a variety of other examples, using measurements performed in both the Arctic and the Antarctic. Some comments and conclusions are given in section 4.

2. Planetary wave cooling, PSC formation and ozone minimum in Arctic winter: an example

The large amplitude of planetary waves in Arctic winter is propitious for adiabatic coolings strong enough to generate PSCs: an uplift of isentropic surfaces of the order of 2000 m will cause air parcels travelling across to cool down by approximately 20 K while conserving their humidity and trace components, and eventually reach temperatures low enough to make possible the generation of Type I or even Type II PSCs. In addition, due to its relatively slow time scale, a planetary wave uplift is able to maintain this low temperature long enough for completing the formation of Type II or even Type I PSCs.

Fig. 1a shows the total ozone distribution on 19 January 1995, as measured by TOVS. A strong minimum around 200 Dobson units is conspicuous, centered on the northern tip of Scandinavia. This minimum can be due to the destruction of ozone by heterogeneous chemistry over PSCs; it can also be directly related to an uplift of air masses which decreases the ozone columnar content by simply decreasing the pressure thickness of the ozone layer without change in the mixing ratio (Salby and Callaghan, 1993); finally, it could be, at least in part, produced by a bias of the TOVS analysis in the presence of a PSC. This case is interesting because PSCs were indeed observed on that day at Sodankylä (67.37°N, 26.65°E) during the SESAME campaign (Pyle et al., 1996; Masci et al., 1996; Wedekind et al., 1996) using multi-wavelength lidars. Wedekind et al. (1996) identify the PSC layer they observe on 19 January 1995 betwen 19.5 and 23.5 km as made of spherical droplets of supercooled ternary solutions (STS) consisting of H_2O, HNO_3 and H_2SO_4. In Figs. 1c to 1g, the cross indicates the location of Sodankylä, where a sounding has been performed on that day (in all the following charts, the cross will indicate the location where a relevant sounding is available).

The sounding performed at Sodankylä on the 19 January shows very strong cooling, down to 186 K, at an altitude of about 22 km (Wedekind et al., 1996). This sounding is consistent with the ECMWF large-scale analysis of the same day temperature field (Fig. 1b); Sodankylä is actually one of the Arctic stations that are routinely used in the ECMWF analysis system. There is thus a strong indication that this cooling is in fact related to the large scale temperature field, and indeed to the planetary wave structure depicted by ECMWF analyses. The ECMWF analysis of geopotential height for the 510 K isentrope is displayed in Fig. 1c, where strong uplift is noticeable over northern Scandinavia and the Kola peninsula, reaching altitudes of the order of 22 km. The corresponding cooling, also from the ECMWF analysis, can be seen in Fig. 1d; it shows that the low temperatures observed over Sodankylä

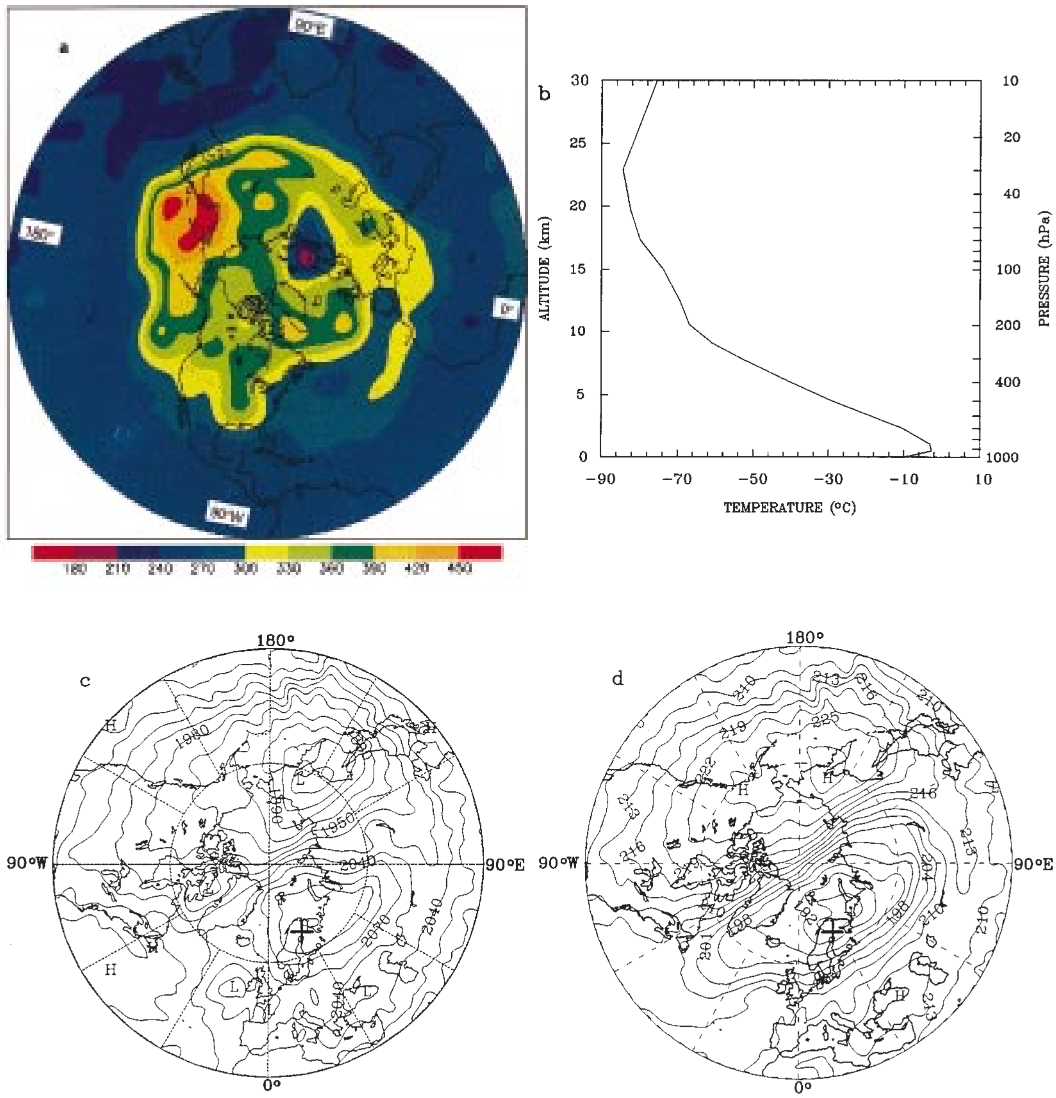

Fig. 1. The case of 19 January 1995 18 UT in the Arctic (a) TOVS total ozone analysis, as retrieved by the Climate Analysis Center (in Dobson units). (b) Large scale vertical temperature profile at Sodankylä, as interpolated from the ECMWF analysis. (c) Geopotential height of the 510 K isentropic surface in dam, as analysed by the ECMWF, with the location of Sodankylä indicated by a cross. (d) Temperature of the 510 K isentropic surface in K, as analysed by the ECMWF. (e) Wavenumber one analysis of the geopotential height of 1c. (f) Wavenumber one analysis of the temperature field of 1d. (g) Montgomery potential from the ECMWF analysis. Note that the TOVS chart is rotated with respect to the standard frame.

extend over a similar region, comprising northern Scandinavia and the Barentz sea. That the phenomenon is indeed related to planetary scale structures is fairly obvious on Figs. 1c and 1d and is further checked by a zonal Fourier analysis; the two fields are overwhelmingly dominated by the wavenumber one component, with amplitudes close to 1300 m for the geopotential height field (Fig. 1e) and 20 K for the temperature field (Fig. 1f). The corresponding values for the original

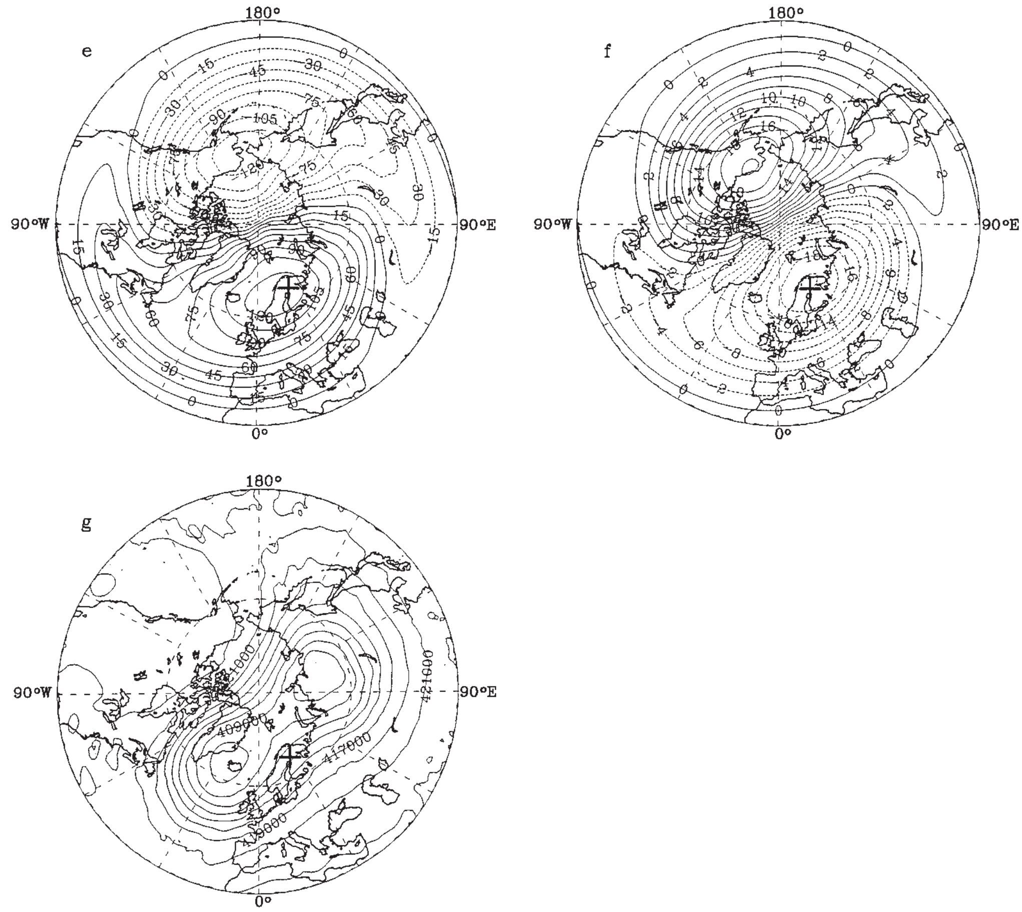

Fig. 1. (*continued*)

fields (obtained by halving the maximum minus minimum values in Figs. 1c, d) are 1800 m and 20 K, respectively; these amplitudes approximately verify the adiabatic relation $c_p \Delta T = -g\Delta z$, which clearly links the cooling to the planetary scale upwelling of isentropic surfaces. The filtered components are shown here to underline the dominance of wavenumber one; but we cannot expect that they exactly retain the phase and amplitude relations that we observe in the original geopotential and temperature fields.

Fig. 1g shows, again from ECMWF analyses, the Montgomery potential or dry static energy $M = c_p T + gz$ (which, after division by the Coriolis parameter, gives the streamfunction of quasigeostrophic velocities along isentropic surfaces). As temperatures and heights along isentropes are negatively correlated, M is a residual that is strongly dominated by wavenumber two. Comparing Fig. 1g to Figs. 1c, 1d, we observe that the streamlines cross both the isotherms and the isolines of the geopotential feld. Sodankylä is under the influence of strong south-westerly winds (of the order of 15 m s^{-1}) coming from warmer, lower portions of the isentropic surface: air parcels are therefore brought to high altitudes and adiabatically cooled by the planetary scale flow. We have not performed back-trajectory calculations, but inspection of the Montgomery potential and temperature charts analysed by ECMWF, 12 h before show that, at that time, cloudy air parcels were already at similar temperatures.

Thus on 19 January 1995, planetary scale conditions were such as to allow the presence of PSCs

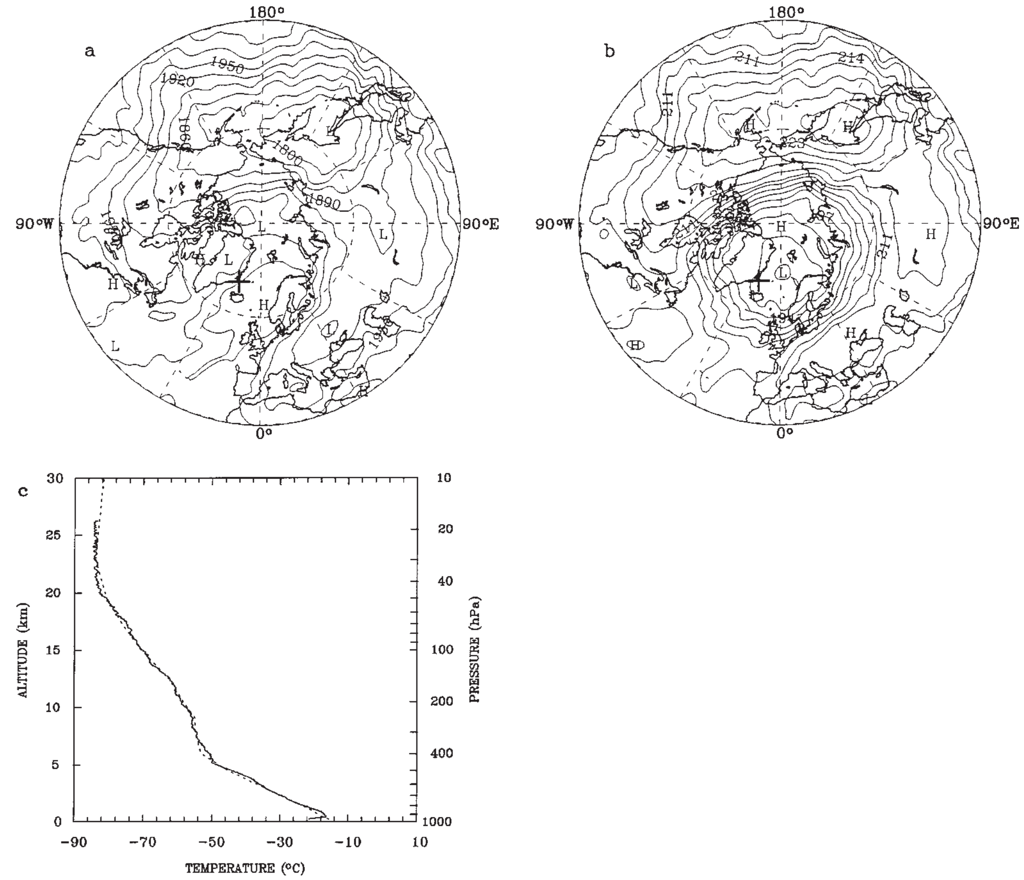

Fig. 2. The case of the 13 January 1995 18 UT in the Arctic. Geopotential height (a) and temperature (b) fields at 485 K (from ECMWF). (c) Comparison of temperature profiles at Scorebysund — observed (continuous line) and interpolated from ECMWF analysis (discontinuous line).

of either type over north-east Scandinavia. The temperature of about 188 K indicated by the Sodankylä sounding is interpreted by the ECMWF analysis as a large scale feature, consistent with the adiabatic cooling implied by the planetary scale uplift of isentropic surfaces.

3. Further examples of PSCs and planetary waves in the arctic and in the Antarctic

We shall show some cases of PSCs which are clearly generated by cooling induced by planetary waves. We shall see that the mechanism is equally valid for the Arctic as well as for the Antarctic regions. In all cases the geopotential and temperature maps will be shown on the isentropic levels nearest to the level where the PSC has been detected. As often as possible we shall compare the measured temperature profile with the one obtained from the ECMWF analysis.

3.1. In the Arctic

We start with a PSC detected during the SESAME campaign like the example shown in the previous section. Backscatter soundings from a balloon launched on the Greenland coast from Scoresbysund (76.5°N, 22.0°W) on 13 January 1995 have been reported by Larsen et al. (1996). The maximum backscatter ratio is found at

19–20 km, indicating a PSC located roughly at the 485 K potential temperature level.

Fig. 2a shows the geopotential field obtained from the ECMWF analysis on the 485 K isentrope. At the sounding place (marked by a cross) the geopotential is relatively high, even though it is not at its maximum. Longitudinal Fourier analysis shows that, with an amplitude of 1200 m, wavenumber one (not shown) is again the main contributor to the deformation of the isentropic surface. Not surprisingly, the temperature variations on the same surface (Fig. 2b) are clearly related to the vertical displacement of the air parcels. Finally in Fig. 2c, we compare the temperature profile obtained from the sounding, with the one obtained from the ECMWF analysis. Like Sodankylä, Scoresbysund is a station routinely used in ECMWF analyses; the agreement between both profiles, though expected, shows that the cooling which generates the PSC is a large scale process

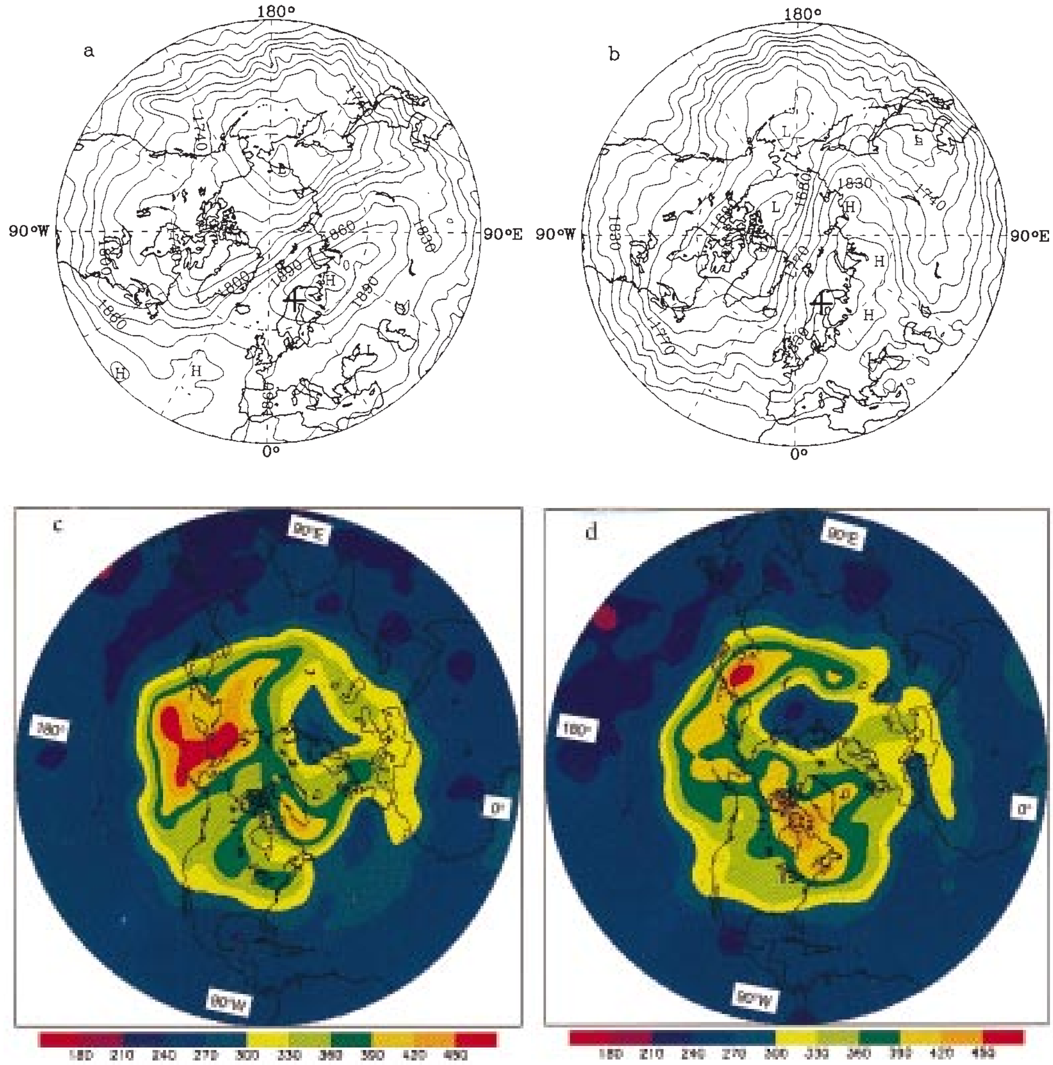

Fig. 3. The case of 21 and 28 January 1995 18 UT in the Arctic. Geopotential height at 460 K on the 21th (a) and on the 28th (b); TOVS total ozone analysis (Climate Analysis Center) for the 21st (c) and for the 28th (d).

rather than a consequence of a localized mountain wave, which the ECMWF model would not be able to resolve.

We shall now compare two different days in which balloon-borne instruments have been launched from Kiruna (67.27°N, 27.65°E) to detect PSCs (Deshler, 1996). In spite of the fact that in both cases (21 and 28 January 1995), the launching site was located inside the vortex (Deshler, 1996), a PSC was detected only on day 21. As we now show, this difference between the two days is related to the planetary wave situation.

Figs. 3a,b show the ECMWF analyses of the geopotential field on 21 and 28 January respectively on the 460 K isentrope. While the site of Kiruna (marked in the figure by a cross) is near a geopotential maximum on the 21st, on the 28th, the geopotential maximum has drifted towards north-central Siberia (again we have verified that wavenumbers one and two are mainly responsible for these situations). The temperature profiles for the two days, obtained from ECMWF analyses (not shown) indicate that the minimum on the 21 January is about -82°C, compared with

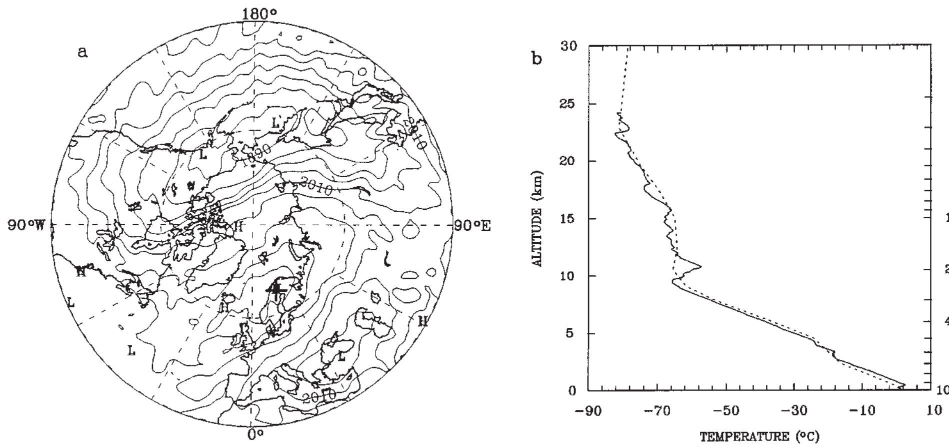

Fig. 4. The case of 11 December 1991 12 UT in the Arctic. Geopotential height at 510 K (a); Kiruna temperature sounding (continuous line) compared to ECMWF analysis (discontinuous line) (b).

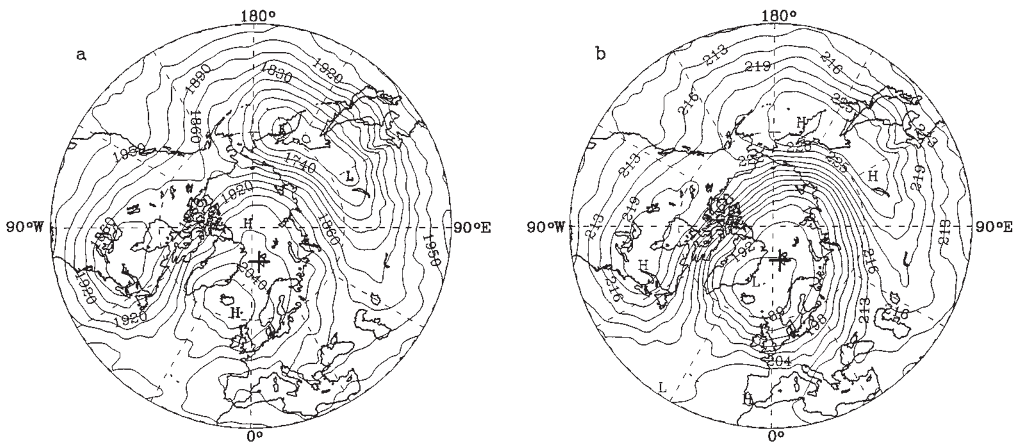

Fig. 5. The case of 14 February 1996 00 UT in the Arctic. Geopotential height (a) and temperature (b) at 485 K.

−77°C on the 28 January; note that, in contrasts to Sodankylä and Scorebysund, the Kiruna soundings were not used by the ECMWF analyses (Hollingsworth, private communication). The total ozone measured by TOVS on both days (Figs. 3c,d) show that the columnar deficit drifts eastward along with the geopotential maximum. As stated above, this effect may be just driven by the upper layer mass depletion effect of Salby and Callaghan (1993), or be related to simultaneous drifting of the PSC along with the temperature minimum, producing either ozone destruction or TOVS biases.

Another interesting case is the PSC detected by an airborne lidar on 11 December 1991 near Kiruna (Godin et al., 1994). The formation of this PSC has been attributed to cooling induced by a montain wave (Godin et al., 1994; Teitelbaum et al., 1996). The geopotential field on the 510 K isentrope for this day is displayed in Fig. 4a. A relatively strong maximum is noticeable over Kiruna (marked by a cross); its height corresponds to the altitude of the observed PSC. The wavenumber one geopotential field (not shown) has also a striking maximum over the Kiruna region. Both the ECMWF analysis and the local sounding (Fig. 4b) indicate a temperature of −80°C around 20 km, cold enough to induce NAT (the correspondance between the two profiles is striking and strongly supports the large scale interpretation, as again the Kiruna sounding was not used in the analysis). Furthermore, as shown in Ovarlez and Ovarlez (1994), both temperature and humidity conditions between 20 and 25 km are favorable to NAT formation. In fact, a mountain wave is present in this region, but its amplitude decreases above 15 km (Teitelbaum et al., 1996); therefore, although we cannot exclude an influence of the mountain wave, it seems difficult, in view of the ECMWF analyses, to believe that it provides the main cooling mechanism for that particular PSC formation.

Some PSC observations have also been made above Ny- Ålesund, Svalbard (79°N, 12°E) with a ground based lidar during winter 1995–1996 (Stebel et al., 1996). On the 13 February 1996 near midnight, the authors observed an enhanced backscatter ratio around 19 km, with a local temperature below the critical temperature for NAT formation, but (as in our first example) above the frost point of ice. The geopotential obtained from the ECMWF analysis (Fig. 5a) shows that the geopotential over Svalbard (marked by a cross), though not at its maximum, is within a large scale uplift area. The temperature chart on the same 485 K isentropic level (Fig. 5b) shows that the low values induced by planetrary waves are well in agreement with the temperature claimed by the authors for the NAT formation.

On 23 January 1996, a Type II PSC (i.e., formed of ice particles) has been observed over Sodankylä by Vömel et al. (1997), using a backscatter sonde. PSCs of type II are especially rare in the Arctic. This time the temperature was very low, below

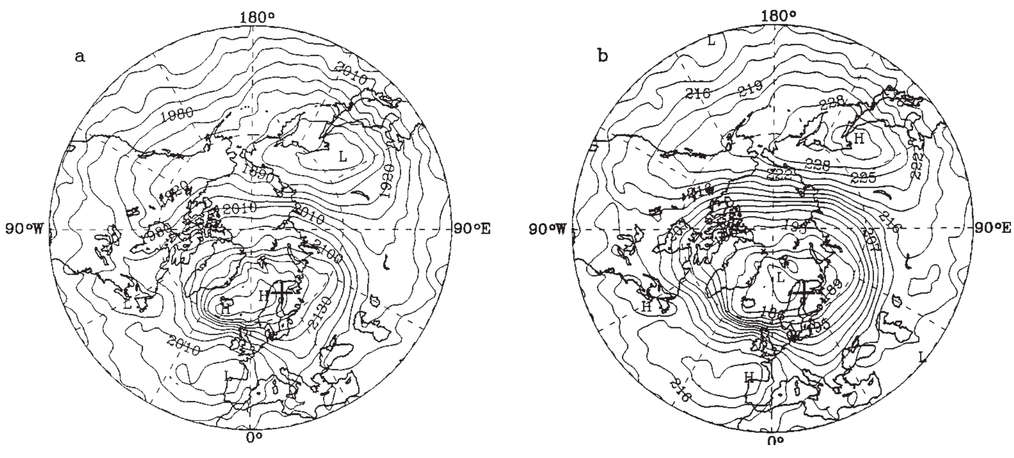

Fig. 6. The case of 23 January 1996 00 UT in the Arctic. Geopotential height (a) and temperature (b) at 510 K.

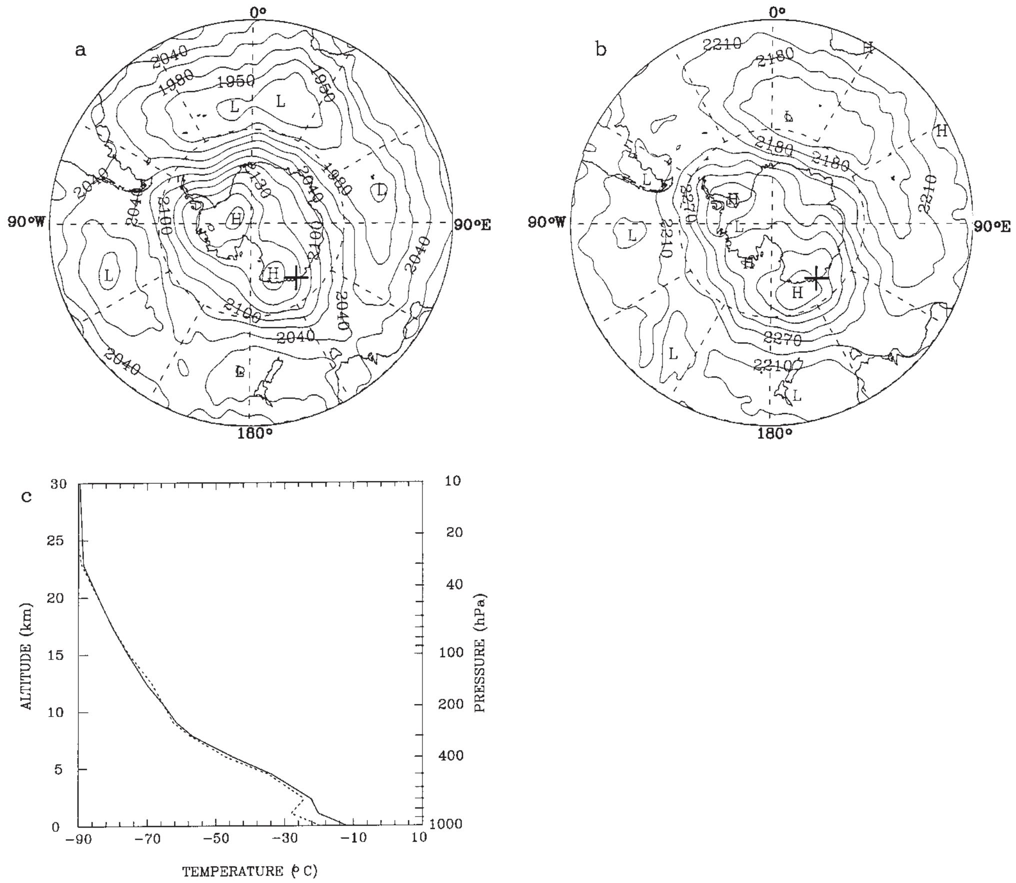

Fig. 7. The case of 7 and 9 July 1992 06 UT in the Antarctic. Geopotential height at 500 K on the 7th (a) and on the 9th (b), together with the ECMWF temperature profiles at Dumont d'Urville (c) on the 7th (continuous line) and on the 9th (dotted line).

the frost point of ice. Furthermore, the existence of the ice cloud was confirmed by a very strong dehydration at the level of the PSC, measured by the same authors with a frost-point hygrometer. Again the ECMWF analysis shows that the cooling induced PSC is due to planetary waves. Fig. 6a shows that the launching site (marked by a cross) is within a strong uplift area. In this case Fourier analysis (not shown) indicates that the exceptionally strong cooling is the result of wavenumbers one and two being in phase over Sodankylä. Once again, the temperature chart (Fig. 6b) agrees with the geopotential variation induced by planetary waves, with a minimum temperature lower than -88° C around 22 km, enough to form a type II PSC.

3.2. In the Antarctic

In the Antarctic we shall refer to measurements performed by a ground based lidar at Dumont d'Urville (67°S, 140°E) described by David (1995). We shall take account of two observations separated by a two day interval, interpreted by the author as a type II PSC, on 7 and 9 July 1992. Fig. 7a shows the ECMWF analysis of the 7 July geopotential height at the 500 K isentropic level. The maximum near the observation site (marked by a cross) is explained by the superposition of wavenumbers 1, 2 and 3 (not shown). Fig. 7b shows the same field for 9 July at 550 K. The temperature profiles, also from ECMWF analysis (Fig. 7c), show that, in both cases, the large scale cooling is indeed adequate for ice PSC formation. The involvement of planetary waves in PSC formation is thus also sustained by observations in the southern hemisphere.

4. Conclusion

In all the cases we have found, the appearance of PSCs of either type is associated with a strong planetary scale upwelling of isentropic surfaces. The associated large scale cooling of adiabatically travelling air parcels is thus an obvious candidate for PSC formation. This would also mean that the probability of presence of PSCs should follow a planetary scale distribution. At present, this possibility is difficult to verify, as we only dispose of isolated samples of PSC detection. An experiment like Stratéole (Vial et al., 1995) would improve our analysis of the problem by providing extensive sampling of the Antarctic vortex by a fleet of constant level drifting balloons, providing both PSC detection and simultaneous, unbiased measurements of the columnar ozone content (Valero et al., 1989).

In any case, studies investigating the link between mountain waves and PSC formation should clearly distinguish between the effect of local disturbances and the effect of the large scale flow structure, as depicted for example by ECMWF analyses.

5. Acknowledgements

We are grateful to ECMWF for providing meteorological analyses for calculation of geopotential, temperature and Montgomery potential fields. The TOVS total ozone analyses were provided by the NOAA Climate Analysis Center.

REFERENCES

Cariolle, D., Muller, S., Cayla, F. and McCormick, M. P. 1989. Mountain waves, polar stratospheric clouds, and the ozone depletion over Antarctica. *J. Geophys. Res.* **94**, 11233–11240.

Crutzen, P. J. and Arnold, F. 1986. Nitric acid cloud formation in the cold Antarctic stratosphere: a major cause of springtime ozone hole. *Nature* **324,** 651–655.

David, C. 1995. *A study of polar stratospheric clouds and volcanic aerosols in polar regions by laser sounding.* PhD Thesis, University of Paris 6 (in French).

Deshler, T. 1996. Vertical profiles of volcanic aerosol and polar stratospheric clouds above Kiruna, Sweden, winter 1995. In: *Polar stratospheric ozone.* Proceedings of the 3rd European Workshop, Schliersee, Germany. Office for official publication of the European Communities 101–104.

Farman, J. C., Gardiner, B. G. and Shanklin, J. D. 1985. Large losses of total ozone in Antarctica reveal seasonal CLOx/NOx interaction. *Nature* **315**, 207–210.

Godin, S., Mégie, G., David, C., Haner, D., Flesia, C. and Emery, Y. 1994. Airborne lidar observations of mountain wave-induced polar stratospheric clouds during EASOE. *Geophys. Res. Lett.* **21,** 1335–1338.

Larsen, N., Knudsen, B., Rosen, J. M. and Kjome, N. T. 1996. PSC formation in the Arctic observed by balloon borne backscatter sondes. In: *Polar stratospheric Ozone.* Proceedings of the 3rd European Workshop, Schliersee, Germany. Office for official publication of the European Communities, 105–108.

Masci, F., Rizi, V., Visconti, G., Wedekind, C., Immler, F., Rairoux, P., Stein, B., Woste, L., del Guasta, M., Morandi, M., Stefanutti, L., Matthey, R., Mitev, V., Douard, M., Wolf, J. P., Kyro, E. and Kivi, R. 1996. Polar stratospheric cloud observations at Sodankylä. In: *Polar stratospheric ozone.* Proceedings of the 3rd European Workshop, Schliersee, Germany. Office for official publication of the European Communities, 126–131.

McCormick, M. P., Chu, W. P., Grams, G. W., Hamill, P., Herman, B. M., McMaster, L. R., Pepin, T. J., Russel, P. B., Steele, H. M. and Swissler, T. J. 1981. High-latitude stratospheric aerosols measured by SAM II satellite system in 1978 and 1979. *Science* **214**, 328–331.

Molina, L. T. and Molina, M. J. 1987. Production of CL_2O_2 from the self reaction of CLO radical. *J. Phys. Chem.* **91**, 433–436.

Molina, M. J., Tsuo, T. L., Molina, L. T. and Wang, F. C. Y. 1987. Antarctic stratospheric chemistry of chlorine nitrate, hydrogen chloride and ice: Release of active chlorine. *Science* **238**, 1253–1257.

Ovarlez, J. and Ovarlez, H. 1994. Stratospheric water vapor content evolution during EASOE. *Geophys. Res. Lett.* **21**, 1235–1238.

Pyle, J. A., Harris, N. R. P. and Amanatidis, G. P. (Editors) 1996. Polar stratospheric ozone. Proceedings of the 3rd European Workshop, Schliersee, Germany. Office for official publication of the European Communities. 890 pp.

Rowland, F. S., Sato, H., Khwaja, H. and Elliot, S. M. 1986. The hydrolysis of chlorine nitrate and its possible atmospheric significance. *J. Phys. Chem.* **90**, 1985–1988.

Salby, M. L. and Callaghan, P. F. 1993. Fluctuations of total ozone and their relationships to stratospheric air motions. *J. Geophys. Res.* **98**, 2715–2727.

Solomon, S., Garcia, R. R., Rowland, F. S., and Wuebbles, D. J. 1986. On the depletion of Antarctic ozone. *Nature* **321**, 755–758.

Stebel, K., Neuber, R., Beyerle, G., Biele, J., Scheuch, P., Schütt, H., von der Gathen, P. and Schrems, O. 1996. Lidar observations of polar stratospheric clouds above Spitsbergen. *Advances in atmospheric remote sensing with lidar*. Selected papers of the 18th International Laser Radar Conference, 509–512.

Teitelbaum, H., Moustaoui, M., Ovarlez, J. and Kelder, H. 1996. The role of atmospheric waves in the laminated structure of ozone profiles at high latitude. *Tellus* **48A**, 442–455.

Tolbert, M. A., Rossi, M. J. and Golden, D. M. 1987. Reaction of chlorine nitrate with hydrogen chloride and water at Antarctic stratospheric temperatures. *Science* **238**, 1258–1260.

Toon, O. B., Hamill, P., Turco, R. P. and Pinto, J. 1986. Condensation of HNO_3 and HCl in the winter polar stratosphere. *Geophys. Res. Lett.* **13**, 1284–1287.

Turco, R. P., Toon, O. B. and Hamill, P. 1989. Heterogeneous physicochemistry of the polar ozone hole. *J. Geophys. Res.* **94**, 16493–16510.

Valero, F. P. J., Ackerman, D. P. and Gore, W. J. Y. 1989. The effect of the Arctic haze as determined from airborne radiometric measurements during AGASP-II. *J. Atmos. Chem.* **9**, 225–244.

Vial, F., Babiano, A., Brioit, B., Basdevant, C., Legras, B., Sadourny, R., Ovarlez, H., Ovarlez, J., Teitelbaum, H., Cariolle, D., Lefévre, F., Simon, P., Valero, F., Mechoso, C., Farrara, J., Kelder, H., Camy-Peyret, C., Hart, T. and McIntyre, M.E., 1995. Stratéole: A project to study Antarctic Polar Vortex dynamics and their impact on ozone chemistry. *Phys. Chem. Earth* **20**, 83–96.

Wedekind, C., Immler, F., Mielke, B., Rairoux, P., Stein, B., Wöste, L., del Guasta, M., Morandi, M., Stefanutti, L., Asci, F., Rizi, V., Matthey, R., Mitev, V., Douard, M., Wolf, J. P. and Kyrö, E. 1996. Lidar observations of liquid and solid PSC at Sodankylä. In: *Polar stratospheric ozone.* Proceedings of the 3rd European Workshop, Schliersee, Germany. Office for official publication of the European Communities, 136–140.

Vömel, H., Rummukainen, M., Kivi, R., Karhu, J., Turunen, T., Kyro, E., Rosen, J., Kjome, N. and Oltmans, S. 1997. Dehydration and sedimentation of ice particles in the Arctic stratospheric vortex. *Geophys. Res. Lett.* **24**, 795–798.